Dalton Transactions

PAPER

View Article Online
View Journal

Cite this: DOI: 10.1039/c5dt01355k

New organically templated thiocyanatocadmates and chlorocuprate(II): synthesis and structural characterization†

Bing Guo,[a] Xiao Zhang,[b] Jie-Hui Yu*[a] and Ji-Qing Xu*[a]

Received 10th April 2015,
Accepted 12th May 2015

DOI: 10.1039/c5dt01355k

www.rsc.org/dalton

With various organic base molecules as the countercations, five new thiocyanatocadmates $[H_2(tmen)][Cd(SCN)_4]$ (tmen = *N*,*N*,*N*′,*N*′-tetramethylethylenediamine) **1**, $[H_2(tmba)][Cd_2(SCN)_6]$ (tmba = *N*,*N*,*N*′,*N*′-tetramethyl-1,4-butanediamine) **2**, $[H_2(teen)][Cd_2(SCN)_6]$ (teen = *N*,*N*,*N*′,*N*′-tetra-ethylethylenediamine) **3**, $[H(amp)][Cd(SCN)_2(CH_3COO)]$ (amp = 2-amino-6-methylpyridine) **4** and $[H(abp)]_4[Cd(SCN)_4]SO_4{\cdot}H_2O$ (abp = 2-amino-6-bromopyridine) **5**, and one new chlorocuprate(II) $[H_2(cha)][CuCl_4]$ (cha = 1,4-cyclohexanediamine) **6** were obtained from a series of simple room-temperature self-assemblies at pH = 2 or 6.5. X-ray single-crystal diffraction analysis reveals that (i) templated by $[(CH_3)_2NH(CH_2)_2NH(CH_3)_2]^{2+}$ ($H_2(tmen)^{2+}$), the anion $[Cd(SCN)_4]^{2-}$ in **1** shows a 1-D linear single-chain structure, whereas templated by $[(CH_3)_2NH(CH_2)_4NH(CH_3)_2]^{2+}$ ($H_2(tmba)^{2+}$), the anion $[Cd_2(SCN)_6]^{2-}$ in **2** shows a 1-D linear double-chain structure. The number of C atoms between the two N atoms in the templating agent controls the width of the anionic chain through the N_{amino}–H···N_{SCN} interactions; (ii) templated by $[(C_2H_5)_2NH(CH_2)_2NH(C_2H_5)_2]^{2+}$ ($H_2(teen)^{2+}$), the anion $[Cd_2(SCN)_6]^{2-}$ in **3** exhibits a 3-D open-framework structure, which is based on zigzag anionic chains. A direct change of the substituent group from $-CH_3$ to $-C_2H_5$ alters indirectly the shape of the anionic chain from a linear shape to a zigzag shape; (iii) **4** shows a 3-D supramolecular network structure, which is built up from the 1-D zigzag anionic structures by the $H(amp)^+$ molecules *via* N–H···O interactions. The formation of the zigzag chain derives from the chelation of the CH_3COO^- groups to the Cd^{2+} centers; (iv) **5** is indeed a double salt of $[H(abp)]_2[Cd(SCN)_4]$ and $[H(abp)]_2SO_4$. SO_4^{2-} and $H(abp)^+$ form a supramolecular aggregation. Surrounded by the aggregations, the anion $[Cd(SCN)_4]^{2-}$ only shows a dinuclear structure; and (v) templated by $H_2(cha)^{2+}$, the anion $[CuCl_4]^{2-}$ in **6** displays a 2-D perovskite layer structure. The photoluminescence analysis indicates that upon excitation (λ_{ex} = 335 nm for **4**, λ_{ex} = 395 nm for **5**), **4** and **5** emit light (λ_{em} = 365 nm for **4**, λ_{em} = 470 nm for **5**), which can be seen clearly under the UV lamp.

Introduction

As an important branch of hybrid inorganic–organic materials, certain attention has been paid to the design and synthesis of novel organically templated halometallates and pseudohalometallates.[1] Over the last thirty years, a number of related hybrid compounds have been obtained using various organic base molecules as the countercations.[2] For example, (i) compound $[H(py)]_2[Cu_3I_5]$ (py = pyridine) is a discrete iodocuprate(I) with the highest core number ($Cu_{36}I_{56}^{20-}$);[3] (ii) compound $[Cu(en)_2]_2[Cu_7I_{11}]$ (en = ethylenediamine) is the first example of 3-D chlorocuprate(I) with the occluded $[Cu(en)_2]^{2+}$ cations;[4] (iii) compound $[H_2(edamp)]_2[Pb_7I_{18}]{\cdot}4H_2O$ (edamp = $Et_2NC_6H_4CH_2C_6H_4NEt_2$) is the unique example of 3-D iodoplumbate with the occluded $H_2(edamp)^{2+}$ cations.[5] The continuous investigation of this field by researchers is generally based on two aims: revealing how the organic cation controls the structure of the inorganic anion, based on the structural information of these hybrid compounds[6] and obtaining some new materials with special properties, which derive from a hybrid formation of two moieties.[7] For instance, (i) the hybrid formation changes the Cu(I)···Cu(I) distance in the halocuprate(I). Those with the short Cu(I)···Cu(I) distances emit green, yellow or red light, while those with the long Cu(I)···Cu(I) distances emit blue light;[8] (ii) the hybrid formation alters the Cu(II)···Cu(II) interaction in the halocuprate(II). Those with the short Cu(II)···Cu(II) interactions may exhibit a ferromagnetic

[a]*College of Chemistry, State Key Laboratory of Inorganic Synthesis and Preparative Chemistry, Jilin University, Changchun, Jilin 130012, China. E-mail: jhyu@jlu.edu.cn, xjq@mail.jlu.edu.cn*

[b]*State Key Lab of Urban Water Resource and Environment (SKLUWRE) & Academy of Fundamental and Interdisciplinary Science, Harbin Institute of Technology, Harbin, Heilongjiang 150080, China*

† Electronic supplementary information (ESI) available. CCDC 1058262–1058267. For ESI and crystallographic data in CIF or other electronic format see DOI: 10.1039/c5dt01355k

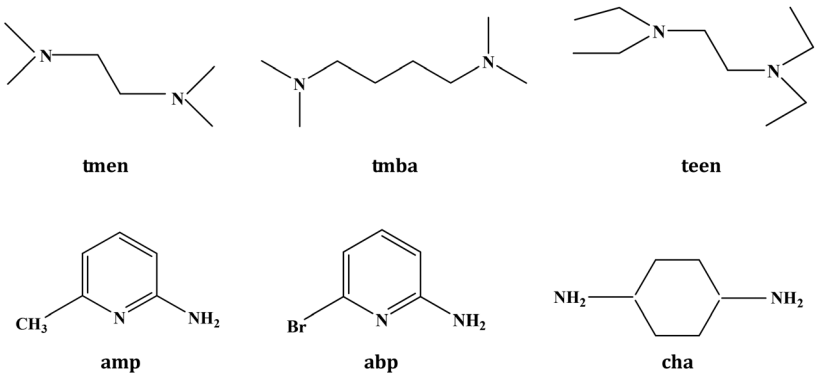

Scheme 1 Structures of amine cations in **1**–**6**.

property;[9] (iii) the hybrid formation makes the viologen-templated chlorobismuthates(III) possess different anionic structures. The anionic size directly influences its photochromic behavior.[10]

Our current investigation is focused on the structural characterization of organically templated thiocyanatocadmates.[11] The templating agents employed are the multidentate N-containing organic base molecules. Some interesting structures have been obtained, such as the 2-D $[H(2,2'\text{-dtdpy})][Cd(SCN)_3]$ (dtdpy = dithiodipyridine)[12] and $[H_2(pdma)][Cd_2(SCN)_4(SO_4)]$ (pdma = 1,4-phenylenedimethanamine),[13] and the 3-D $[(Hdabco)_2Cd_3(SCN)_8]$ (dabco = 1,4-diazabicyclo-[2,2,2]octane)[14] and $[H_2(tmen)][Cd_3Cl_6(SCN)_2]$ (tmen = *N*,*N*,*N*′,*N*′-tetramethylethylenediamine).[15] Moreover, some interesting phenomena have also been observed. For instance, the anion of the Cd^{2+} precursor can sometimes appear in the final anionic framework.[16] In our latest report, based on the structural information of compound $[H(ba)]_2[CdCl_2(SCN)_2]$ (ba = *tert*-butylamine) and $[H_2(tmen)][Cd_3Cl_6(SCN)_2]$, we give two possible reasons. One is the special arrangement between $-NH_3^+$ and Cl^-, making the supramolecular packing more stable. The other is due to the formation of the Cd–Cl oligomer. The SCN^- groups only displace the Cl^- ions on the outside of the Cd–Cl oligomer, so the Cl^- ions on the inside are retained.[15] In this article, five new organic base molecules (*N*,*N*,*N*′,*N*′-tetramethylethylenediamine (tmen), *N*,*N*,*N*′,*N*′-tetramethyl-1,4-butanediamine (tmba), *N*,*N*,*N*′,*N*′-tetra-ethylethylenediamine (teen), 2-amino-6-methylpyridine (amp), and 2-amino-6-bromopyridine (abp)) were selected to continue preparing the organically templated thiocyanatocadmates. Considering that the organically templated halocuprate(II) possesses diverse structures and nice magnetic properties,[9,17] we also employ the multidentate N-containing organic base molecules to construct the novel halocuprate(II). Fortunately, from a series of simple room-temperature reactions at pH = 2 or 6.5, six new hybrid Cd^{2+} and Cu^{2+} compounds were obtained, including five thiocyanatocadmates: $[H_2(tmen)][Cd(SCN)_4]$ **1**, $[H_2(tmba)][Cd_2(SCN)_6]$ **2**, $[H_2(teen)][Cd_2(SCN)_6]$ **3**, $[H(amp)][Cd(SCN)_2(CH_3COO)]$ **4**, and $[H(abp)]_4[Cd(SCN)_4]$-$SO_4{\cdot}H_2O$ **5**, as well as one chlorocuprate(II) $[H_2(cha)][CuCl_4]$ (cha = 1,4-cyclohexanediamine) **6**. Scheme 1 illustrates the molecular structures of organic bases in the title compounds.

Experimental

Materials and physical measurement

All chemicals are of reagent grade quality, obtained from commercial sources and used without further purification. Elemental analysis (C, H and N) was performed on a Perkin-Elmer 2400LS II elemental analyzer. Infrared (IR) spectra were obtained on a Perkin Elmer Spectrum 1 spectrophotometer in the 4000–400 cm^{-1} region using powdered samples on KBr plates. Powder X-ray diffraction (XRD) data were collected on a Rigaku/max-2550 diffractometer with Cu-K_α radiation (λ = 1.5418 Å). TG behavior was investigated on a Perkin-Elmer TGA-7 instrument with a heating rate of 10 °C min^{-1} in air. Fluorescence spectra were obtained on a LS 55 florescence/phosphorescence spectrophotometer at room temperature. Ultraviolet-visible (UV-vis) spectra were obtained on a Rigaku-UV-3100 spectrophotometer.

Synthesis of title compounds

$[H_2(tmen)][Cd(SCN)_4]$ 1. A solution of tmen (0.1 ml) in C_2H_5OH (3 ml) was carefully layered over an aqueous solution (5 ml) of a mixture of $3CdSO_4{\cdot}8H_2O$ (257 mg, 1 mmol) and NH_4SCN (152 mg, 2 mmol). A few drops of dilute H_2SO_4 were added to acidify the solution to pH = 2. The colorless needle crystals of **1** were obtained after *ca.* 50 days of slow evaporation. Yield: *ca.* 30% based on Cd(II). Anal. Calcd for $C_{10}H_{18}N_6S_4Cd$ **1**: C 25.94, H 3.92, N 18.15. Found: C 25.83, H 3.93, N 17.67%. IR (cm^{-1}): 2100 s, 1465 m, 1398 m, 1332 w, 1152 m, 1056 m, 928 m, 923 w, 773 w, 514 w.

$[H_2(tmba)][Cd_2(SCN)_6]$ 2. A solution of tmba (0.1 ml) in C_2H_5OH (3 ml) was carefully layered over an aqueous solution (5 ml) of a mixture of $3CdSO_4{\cdot}8H_2O$ (257 mg, 1 mmol) and NH_4SCN (152 mg, 2 mmol). A few drops of dilute HCl were added to acidify the solution to pH = 2. The colorless needle crystals of **2** were obtained after *ca.* 6 days of slow evaporation. Yield: *ca.* 25% based on Cd(II). Anal. Calcd for $C_{14}H_{22}N_8S_6Cd_2$

Table 1 Crystal data of **1–6**

	1	2	3	4	5	6
Formula	$C_{10}H_{18}N_6S_4Cd$	$C_{14}H_{22}N_8S_6Cd_2$	$C_{16}H_{26}N_8S_6Cd_2$	$C_{10}H_{12}N_4O_2S_2Cd$	$C_{24}H_{26}N_{12}O_5S_5Br_4Cd$	$C_6H_{16}N_2CuCl_4$
M	462.99	719.64	747.63	396.76	1154.93	321.56
T (K)	293(2)	293(2)	293(2)	293(2)	293(2)	293(2)
Crystal system	Triclinic	Triclinic	Monoclinic	Monoclinic	Triclinic	Monoclinic
Space group	$P\bar{1}$	$P\bar{1}$	$P2_1/c$	$P2_1/c$	$P\bar{1}$	$P2_1/c$
a (Å)	5.9229(12)	5.9186(12)	10.5331(6)	11.1025(7)	9.9159(4)	9.3655(6)
b (Å)	8.1307(16)	10.709(2)	11.2159(6)	10.9745(5)	12.9791(8)	7.2877(5)
c (Å)	10.051(2)	10.863(2)	15.0643(7)	12.9968(6)	16.8359(8)	8.6164(7)
α (°)	107.23(3)	73.96(3)			68.545(3)	
β (°)	97.19(3)	76.92(3)	128.416(3)	103.624(4)	88.854(3)	92.869
γ (°)	93.76(3)	81.30(3)			79.115(4)	
V (Å^3)	455.97(16)	641.6(2)	1394.41(13)	1539.03(14)	1977.49(17)	587.36(7)
Z	1	1	2	4	2	2
D_c (g cm^{-3})	1.686	1.862	1.781	1.712	1.940	1.818
μ (mm^{-1})	1.656	2.164	1.995	1.692	4.908	2.728
Reflections collected	4145	6297	7690	8461	1124	3235
Unique reflections	2039	2912	2457	2713	11 231	1056
R_{int}	0.0217	0.0270	0.0583	0.0212	0.0317	0.0326
Gof	1.070	1.147	1.198	1.050	1.084	1.129
R_1, $I > 2\sigma(I)$	0.0550	0.0339	0.0329	0.0221	0.0603	0.0453
wR_2, all data	0.2145	0.1123	0.0859	0.0547	0.1893	0.1175

2: C 23.37, H 3.08, N 15.57. Found: C 23.55, H 3.04, N 15.25%. IR (cm^{-1}): 2131 s, 2108 s, 1477 m, 1375 m, 1158 w, 1044 w, 1002 w, 953 w, 833 w, 743 w.

[H$_2$(teen)][Cd$_2$(SCN)$_6$] 3. A solution of teen (0.1 ml) in C_2H_5OH (3 ml) was carefully layered over an aqueous solution (5 ml) of a mixture of $CdBr_2{\cdot}4H_2O$ (344 mg, 1 mmol) and NH_4SCN (152 mg, 2 mmol). A few drops of dilute H_2SO_4 were added to acidify the solution to pH = 2. The colorless needle crystals of **3** were obtained after *ca.* 7 days of slow evaporation. Yield: *ca.* 20% based on Cd(II). Anal. Calcd for $C_{13}H_{26}N_5S_3Cd$ **3**: C 25.70, H 3.51, N 14.99. Found: C 25.29, H 3.59, N 14.28%. IR (cm^{-1}): 2131 w, 2116 s, 2050 s, 1471 m, 1447 m, 1393 w, 1351 w, 1278 w, 1098 w, 1037 w.

[H(amp)][Cd(SCN)$_2$(CH$_3$COO)] 4. A solution of amp (108 mg, 1 mmol) in CH_3OH (3 mL) was added slowly to an aqueous solution (5 mL) of a mixture of $Cd(CH_3COO)_2{\cdot}2H_2O$ (267 mg, 1 mmol) and NH_4SCN (152 mg, 2 mmol). A few drops of dilute $NH_3{\cdot}H_2O$ were added to neutralize the solution to pH = 6.5. The mixture was stirred for *ca.* 2 days, and then filtered. The light-yellow needle crystals of **4** were obtained after *ca.* 7 days of slow evaporation from the filtrate. Yield: *ca.* 30% based on Cd(II). Anal. Calcd for $C_{10}H_{12}N_4O_2S_2Cd$ **4**: C 30.27, H 3.05, N 14.12. Found: C 30.45, H 3.17, N 14.22%. IR (cm^{-1}): 2129 w, 2108 s, 1669 s, 1530 s, 1416 m, 1308 w, 1176 w, 1002 w, 785 m, 713 m.

[H(abp)]$_4$[Cd(SCN)$_4$]SO$_4{\cdot}$H$_2$O 5. A solution of abp (173 mg, 1 mmol) in CH_3OH (3 mL) was added slowly to an aqueous solution (5 mL) of a mixture of $Cd(CH_3COO)_2{\cdot}2H_2O$ (267 mg, 1 mmol) and NH_4SCN (152 mg, 2 mmol). A few drops of dilute H_2SO_4 were added to acidify the solution to pH = 2. The mixture was stirred for *ca.* 2 days, and then filtered. The light-yellow needle crystals of **5** were obtained after *ca.* 30 days slow evaporation from the filtrate. Yield: *ca.* 25% based on Cd(II). Anal. Calcd for $C_{24}H_{26}N_{12}O_5S_5Br_4Cd$ **5**: C 24.96, H 2.27, N 14.55. Found: C 25.14, H 2.50, N 14.89%. IR (cm^{-1}): 2123 w, 2096 m, 2033 s, 1657 s, 1596 m, 1466 w, 1375 w, 1306 w, 1094 m, 1078 s, 982 m, 797 w, 710 w.

[H$_2$(cha)][CuCl$_4$] 6. A solution of cha (114 mg, 1 mmol) in C_2H_5OH (3 ml) was carefully layered over an aqueous solution (5 ml) of $CuCl_2{\cdot}2H_2O$ (341 mg, 2 mmol). A few drops of dilute H_2SO_4 were added to acidify the solution to pH = 2. The green needle crystals of **6** were obtained after *ca.* six months of slow evaporation. Yield: *ca.* 15% based on Cu(II). Anal. Calcd for $C_6H_{16}N_2CuCl_4$ **6**: C 22.41, H 5.02, N 8.71. Found: C 22.43, H 4.94, N 8.67%. IR (cm^{-1}): 1603 s, 1559 w, 1438 s, 1435 w, 1398 m, 1284 w, 1128 m, 1086 w.

X-ray crystallography

The data were collected with Mo-K$_\alpha$ radiation (λ = 0.71073 Å) on a Rigaku R-AXIS RAPID IP diffractometer for compounds **1** and **2**, and on a Siemens SMART CCD diffractometer for compounds **3–6**. With the SHELXTL program, the structures of compounds **1–6** were all solved using direct methods.[18] The non-hydrogen atoms were assigned anisotropic displacement parameters in the refinement, and other hydrogen atoms were treated using a riding model. The hydrogen atoms on N4 in compound **2**, N4 in compound **3**, and N1 in compound **6** were obtained from the difference Fourier map. The hydrogen atoms on N3 in compound **1** and on Ow1 in compound **5** were not located. The abp IV in compound **5** suffered from severe disorder, so the AFIX 66 instruction was employed to fix the pyridine ring and anisotropic refinement was not carried out for the disordered atoms. As a result, a larger Q peak around the disordered atoms appeared. The structures were then refined on F^2 using SHELXL-97.[18] CCDC numbers are 1058262–1058267 for compounds **1–6**. The crystallographic data for the title compounds are summarized in Table 1.

Results and discussion

Synthetic analysis

All the reactions were carried out under ambient conditions. All of the title hybrid compounds were obtained from acidic environments. On the one hand, the H^+ ion can aid the reactive precursors to dissolve quickly in the solvents to form a clear solution. The single crystals grow easily from a clear solution. On the other hand, the acidic environment can ensure that the organic base is completely protonated. It can be noted that the amino-substituted pyridine molecules show an exceptional situation. The pyridyl N atom is found to be easily protonated. For example, the pyridyl N is found to have been protonated at pH = 6.5, based on the preparation of compound **4**. However, the amino group is generally not protonated, even when pH = 2, based on the preparation of compounds **4**, **5** and [H(apy)][Cd(SCN)$_3$] (apy = 4-aminopyridine) reported previously.[15] H_2SO_4 can act as the H^+ resource but sometimes the SO_4^{2-} group can be mixed into the final framework, as observed in compound **5**. This situation has also been encountered in past investigations, producing the hybrid compounds $[H_2(pip)]_4[Cd_3Br_8(SCN)_2(SO_4)_2(H_2O)]\cdot 4H_2O$ (pip = piperazine), $[H_2(bim)][Cd(SCN)_2(H_2O)_2]SO_4$ (bim = 2,2′-biimidazole), $[H_2(pympip)]_2[Cd_2(SCN)_4(SO_4)_2(H_2O)_4]\cdot 2H_2O$ (pympip = 1-(2-pyrimidyl)piperazine), $[H_2(pdma)][Cd_2(SCN)_4(SO_4)]$, and $[H_2(4,4'\text{-dtdpy})]_2[CdBr_4]SO_4\cdot 2.5H_2O$ (dtdpy = dithiodipyridine). Only when preparing compound **4**, the anion (CH_3COO^-) for the Cd^{2+} salt appears in the resulting framework. In fact, only in the limited example, the CH_3COO^- group is mixed in the final Cd–SCN backbone.[15] As the anion of the Cd^{2+} salt, the X^- ion (X^- = Cl^-, Br^-) appears frequently in the resulting Cd–SCN framework, creating some new thiocyanatocadmates with interesting structures. Typical examples are $[H_2(dabco)]_2[Cd_3Cl_8(SCN)_2]\cdot H_2O$, $[H_2(pip)][CdCl_3(SCN)]\cdot 2H_2O$[16d] and [CdI(SCN)L] (L = SC(–OC_2H_5)═NH_2).[16c] Moreover, with different acids as the H^+ resource, distinct products are probably obtained. For instance, acidified by H_2SO_4, compound **3** is obtained, while acidified by HBr, compound $[H_2(teen)][CdBr_4]$, a mononuclear compound, is obtained.[19] In the past five years, we employed various organic base molecules to serve as countercations in the self-assembling of a series of thiocyanatocadmates. In this article, we attempt to use these organic bases to construct new halocuprates(II) for the first time and a chlorocuprate(II) **6** has now been obtained.

Structural description

$[H_2(tmen)][Cd(SCN)_4]$ 1. X-ray single-crystal diffraction analysis reveals that compound **1** is a chained thiocyanatocadmate with $H_2(tmen)^{2+}$ as the countercation. The asymmetric unit of compound **1** is found to be composed of a half Cd^{2+} ion (Cd1), two types of SCN^- groups (SCN I labeled as $S_{(1)}C_{(1)}N_{(1)}$, SCN II labeled as $S_{(2)}C_{(2)}N_{(2)}$), and a half $H_2(tmen)^{2+}$ cation. Fig. 1 plots the 2-D supramolecular layer network of compound **1**. Templated by $H_2(tmen)^{2+}$, the SCN I groups double bridge the Cd^{2+} centers into a 1-D endless single chain (see Fig. S1† for better understanding). Since two terminal SCN II groups around each Cd^{2+} center adopt a *trans*-configuration arrangement, the chain shows a linear shape (∠Cd···Cd···Cd = 180°). The chain can also be described as a linear arrangement of the 8-membered $Cd_2(SCN)_2$ loops along the *a*-axial direction. The $Cd_2(SCN)_2$ loop adopts a chair-shape arrangement (mean deviation: 0.1570 Å), making the chain more stable. The Cd1···Cd1d distance is 5.923 Å. The $H_2(tmen)^{2+}$ cations occupy the space between the chains. *Via* the N_{tmen}–H···N_{SCN} interactions (N2···N3e = 2.807 Å), the $H_2(tmen)^{2+}$ cations extend the 1-D $Cd(SCN)_4^{2-}$ chains into a 2-D supramolecular network. Cd1 is in an octahedral site, surrounded by four SCN^- S atoms (S1, S1c, S2, S2c; Cd1–S = 2.711(2)–2.763(2) Å) and two SCN^- N atoms (N1a, N1b; Cd1–N = 2.296(7) Å).

$[H_2(tmba)][Cd_2(SCN)_6]$ 2. Compound **2** is a ribboned thiocyanatocadmate with $H_2(tmba)^{2+}$ as the countercation. The asymmetric unit of compound **2** is found to be composed of one Cd^{2+} ion (Cd1), three types of SCN^- groups (SCN I labeled as $S_{(1)}C_{(1)}N_{(1)}$, SCN II labeled as $S_{(2)}C_{(2)}N_{(2)}$, SCN III labeled as $S_{(3)}C_{(3)}N_{(3)}$) and a half $H_2(tmba)^{2+}$ cation. As shown in Fig. 2, compound **2** possesses a similar supramolecular network

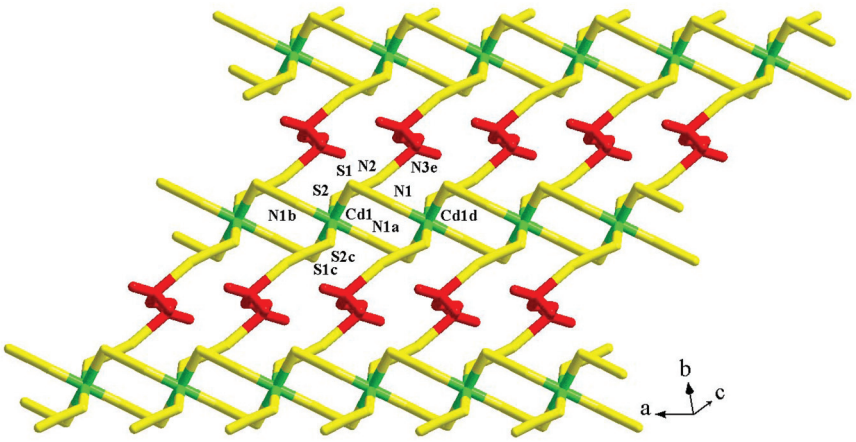

Fig. 1 2-D supramolecular layer network of **1** (a: –*x* + 2, –*y* + 2, –*z*; b: *x* – 1, *y*, *z*; c: –*x* + 1, –*y* + 2, –*z*; d: *x* + 1, *y*, *z*; e: *x*, *y* + 1, *z*).

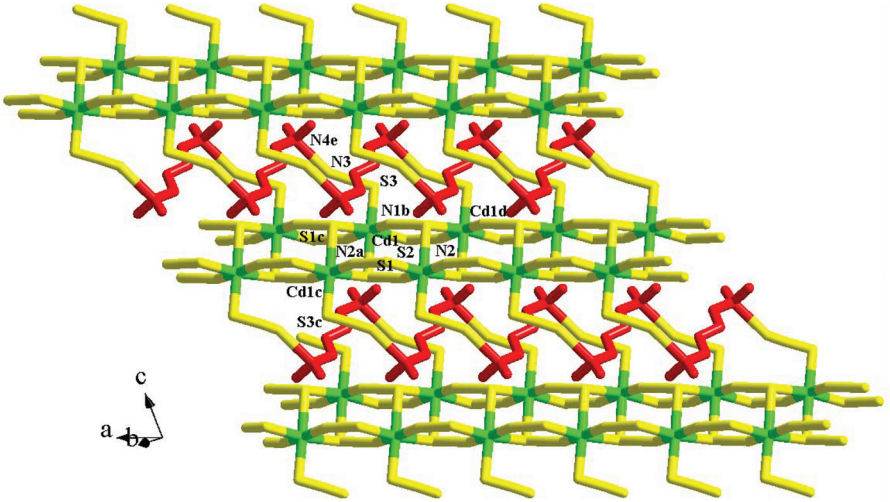

Fig. 2 2-D supramolecular layer network of **2** (a: $x + 1, y, z$; b: $-x + 1, -y + 1, -z$; c: $-x + 2, -y + 1, -z$; d: $x - 1, y, z$; e: $x + 1, y, z$).

structure to that of compound **1**. The difference is that the inorganic anion for compound **2** exhibits a 1-D ribbon structure, templated by $H_2(tmba)^{2+}$ (see Fig. S2† for a better understanding). This ribbon can indeed be regarded as a stacking of two single chains. The terminal SCN^- groups on one side of each single chain are displaced by a set of double-bridged SCN^- S atoms of another single chain finally producing this ribbon. At the same time, a type of triple-bridged SCN^- group forms, namely, SCN I. The octahedral Cd1 is still completed by two N atoms (N1b, N2a; Cd1–N = 2.273(3)–2.300(3) Å) and four S atoms (S1, S2, S3, S1c; Cd1–S = 2.6292(13)–2.8739(13) Å), but two S atoms (S1, S1c) are from the triple-bridged SCN^- groups. The shortest Cd···Cd distance is Cd1···Cd1c = 4.194 Å. The organic amine cations still serve as the bridge in compound **2**, propagating the 1-D infinite ribbons into a 2-D supramolecular layer network *via* the N_{tmba}–H···N_{SCN} interactions (N3···N4e = 2.841 Å).

$[H_2(teen)][Cd_2(SCN)_6]$ 3. Compound **3** is a 3-D thiocyanatocadmate with occluded $H_2(teen)^{2+}$ cations. The asymmetric unit of compound **3** is found to be composed of one Cd^{2+} ion (Cd1), three types of SCN^- groups (SCN I labeled as $S_{(1)}C_{(1)}N_{(1)}$, SCN II labeled as $S_{(2)}C_{(2)}N_{(2)}$, SCN III labeled as $S_{(3)}C_{(3)}N_{(3)}$) and one half of a $H_2(teen)^{2+}$ cation. As shown in Fig. 3c, templated by $H_2(teen)^{2+}$, the inorganic anion exhibits a 3-D network structure, which is based on the 1-D single chains. The SCN I and SCN III groups double bridge the octahedral Cd1 centers to form this 1-D singe chain. Different from the situation observed in compound **1**, this 1-D single chain shows a zigzag shape, since two symmetry-related SCN II groups around each Cd1 center adopt a *cis*-configuration (see Fig. 3a). The zigzag shape is characterized by two structural factors: (i) the Cd···Cd···Cd angle of 124°, and (ii) the dihedral angle (89.1°) between two adjacent $Cd_2(SCN)_2$ loop planes. Since the *cis*-mode $Cd(SCN)_2$ units are alternately distributed on both sides of the zigzag chain, each single zigzag chain has a chance to interact with the neighboring four single zigzag chains (N2, N2b, S2c, S2d acting as the donors), finally forming the 3-D network of compound **3** with the 1-D channels (see Fig. 3b). The $H_2(teen)^{2+}$ cations occlude the channels. The octahedral Cd1 center is surrounded by three SCN^- S atoms (S1, S2, S3; Cd1–S = 2.6898(9)–2.7181(8) Å), and three SCN^- N atoms (N1a, N2c, N3b; Cd1–N = 2.286(3)–2.466(3) Å). Three types of SCN^- groups all adopt a double-bridged coordination mode. Two types of $Cd_2(SCN)_2$ loops are nearly planar with the smaller mean deviations (0.0554 Å for $Cd_2(SCN_{(I)})_2$, 0.0674 Å for $Cd_2(SCN_{(III)})_2$). The Cd1···Cd1a separation is 5.953 Å.

$[H(amp)][Cd(SCN)_2(CH_3COO)]$ 4. Compound **4** is a chained thiocyanatocadmate with $H(amp)^+$ as the countercation. CH_3COO^- appears in the final framework of compound **4**. The asymmetric unit of compound **4** is found to be composed of one Cd^{2+} ion (Cd1), two types of SCN^- groups (SCN I labeled as $S_{(1)}C_{(1)}N_{(1)}$, SCN II labeled as $S_{(2)}C_{(2)}N_{(2)}$), one CH_3COO^- group, and one amp molecule. The amp should be monoprotonated in order to balance the anionic charge, although it has a potential to be diprotonated. Two structural factors determine that the pyridyl N atom is protonated, while the amine N atom is non-protonated. (i) The N3···O1c distance of 2.811 Å implies that there exists a hydrogen-bond interaction between the pyridyl N atom and one CH_3COO^- O atom (see Fig. 4c). (ii) Based on the difference Fourier map, two Q atoms around the amine N atom (N4) for amp are found. The QN4Q angle of *ca.* 120° indicates that N4 is in a planar trigonal site. The zigzag single chain is also observed in compound **4** (∠Cd···Cd···Cd = 142°), but here its formation is due to the chelation of the CH_3COO^- group (see Fig. 4b and S3†). The octahedral Cd1 is coordinated by two SCN^- N atoms (N1b, N2a; Cd1–N1 = 2.307(2)–2.351(2) Å), two SCN^- S atoms (S1, S2; Cd1–S = 2.6043(8)–2.6300(8) Å) and two CH_3COO^- O atoms (O1, O2; Cd1–O = 2.346(2)–2.432(2) Å). The $Cd_2(SCN)_2$ ring is nearly planar (mean deviation: 0.0840 Å), and the Cd1···Cd1a separation is 5.837 Å. As shown in Fig. 4a, *via* the two types of hydrogen-bonded interactions (N3···O1c = 2.811 Å, N4···O2 = 2.837 Å),

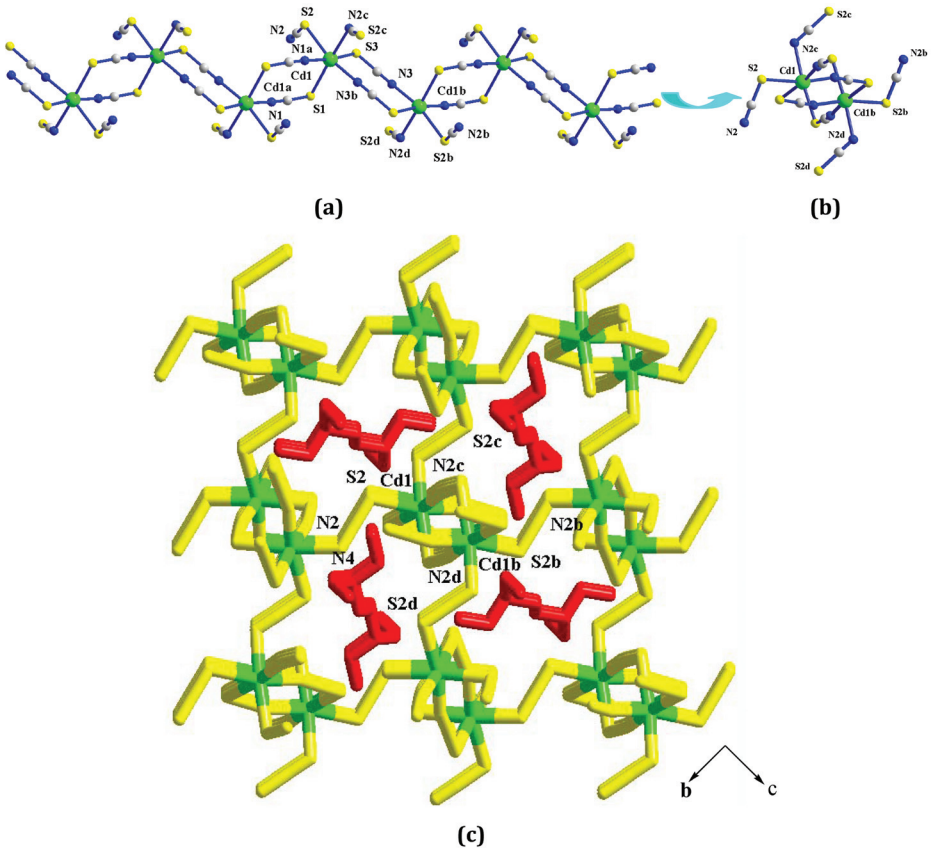

Fig. 3 (a, b) 1-D zigzag chain and (c) 3-D open framework with occluded $H_2(teen)^{2+}$ cations for **3** (a: $-x + 1, -y, -z - 1$; b: $-x, -y, -z - 1$; c: $-x + 1, y + 1/2, -z - 1/2$).

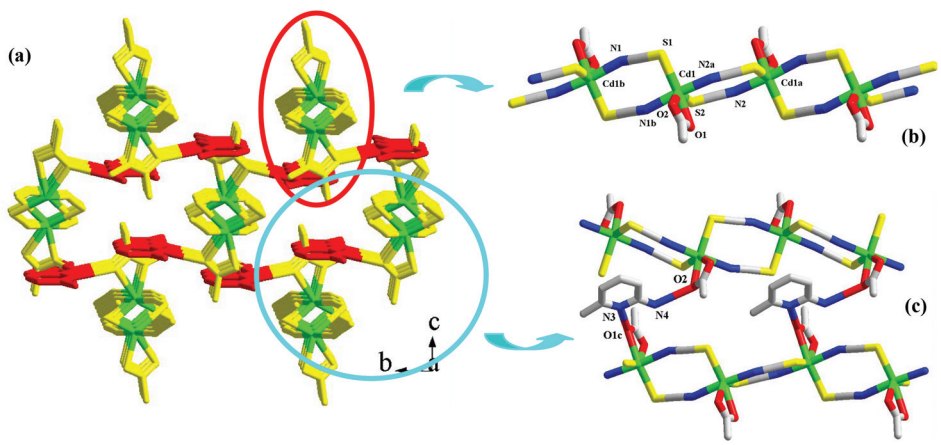

Fig. 4 (a) 3-D supramolecular network, (b) 1-D zigzag chain, and (c) hydrogen-bonded interactions in **4** (a: $-x + 2, -y - 1, -z + 1$; b: $-x + 1, -y - 1, -z + 1$; c: $-x + 1, y + 1/2, -z + 1/2$).

the amp cations act as the bridges, linking the neighboring zigzag chains into a 3-D supramolecular network. Similar to the situation observed in compound **3**, the formation of the 3-D supramolecular network of compound **4** is due to two structural factors: (i) a zigzag shape for the 1-D single chain; (ii) an alternating arrangement on both sides of the chain for CH_3COO^-.

$[H(abp)]_4[Cd(SCN)_4]SO_4 \cdot H_2O$ 5. Compound **5** is indeed a double salt of $[H(abp)]_2[Cd(SCN)_4]$ and $[H(abp)]_2SO_4$. The asymmetric unit of compound **5** is found to be composed of

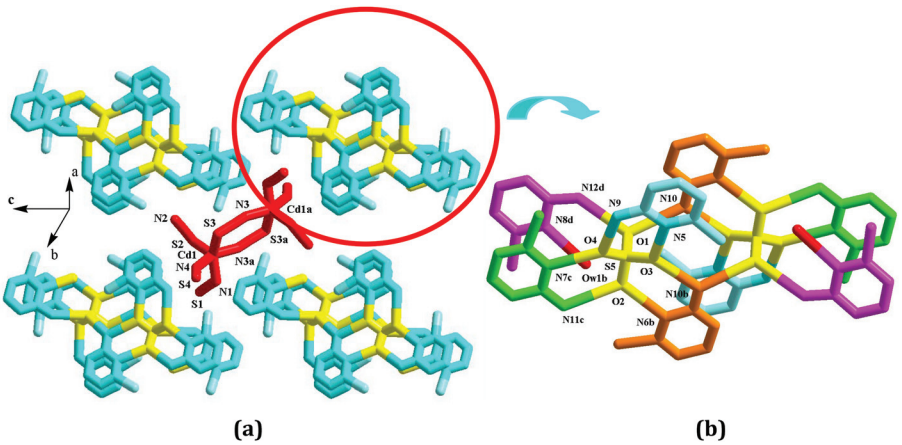

Fig. 5 (a) Packing plot, and (b) supramolecular aggregation constructed from SO_4^{2-}, $H(abp)^+$ and H_2O in **5** (a: $-x, -y + 2, -z + 1$; b: $-x, -y + 1, -z$; c: $-x + 1, -y + 1, -z + 1$; d: $-x, -y + 1, -z + 1$).

one Cd^{2+} ion (Cd1), four types of SCN^- groups (SCN I labeled as $S_{(1)}C_{(1)}N_{(1)}$, SCN II labeled as $S_{(2)}C_{(2)}N_{(2)}$, SCN III labeled as $S_{(3)}C_{(3)}N_{(3)}$, SCN IV labeled as $S_{(4)}C_{(4)}N_{(4)}$), four types of $[H(abp)]^+$ cation (abp I, abp II, abp III, abp IV), one SO_4^{2-} group and one lattice water molecule (Ow1). All of the abp molecules in compound **5** are monoprotonated, in order to balance the systematic charge. As shown in Fig. 5b, *via* a type of hydrogen-bonded synthon ($R_2^2(6)$), the SO_4^{2-} group with three O atoms (O2, O3, O4) as the donors links abp I, abp II and abp III into a supramolecular aggregation (O···N = 2.685–2.902 Å). The fourth O atom (O1) from SO_4^{2-} forms a hydrogen bond to N10 (O1···N10 = 2.911 Å), linking two such aggregations together. Two abp IV molecules (purple) and two water molecules (red) are also mixed into this aggregation *via* the O1···N12d and Ow1b···N8d interactions (O1···N12d = 2.869 Å; Ow1b···N8d = 2.702 Å), finally producing a new supramolecular aggregation. Surrounded by four aggregations, the anion $[Cd(SCN)_4]^{2-}$ only shows a dinuclear structure, as shown in Fig. 5a. Cd1 is in a distorted rectangular pyramidal site, coordinated by three SCN^- N atoms (N1, N4, N3a; Cd1–N = 2.271(7)–2.323 (7) Å) and two SCN^- S atoms (S2, S3; Cd1–S = 2.554(2)–2.630(2)). *Via* an inversion center, the dinuclear structure of compound **5** is completed. SCN III shows a double-bridged mode, whereas SCN I, II and IV adopt the terminal mode. The $Cd_2(SCN)_2$ loops are almost planar (mean deviation: 0.0714 Å), and the Cd1···Cd1a contact distance is 5.904 Å (see Fig. S4† for better understanding).

$[H_2(cha)][CuCl_4]$ 6. Compound **6** is a layered chlorocuprate(II) with $H_2(cha)^{2+}$ as the countercation. The asymmetric unit of compound **6** is found to be composed of one half of a Cu^{2+} ion (Cu1), two types of Cl^- ions (Cl1, Cl2) and one half of a $H_2(cha)^{2+}$ cation. As shown in Fig. 6b, Cu1 is involved in a square planar site, surrounded by four Cl^- ions (Cl1, Cl2, Cl1a, Cl2a). The Cu1–Cl range is 2.2726(7)–2.2983(8) Å. In fact, the divalent Cu ion with a square coordination geometry is rather rare. On the axial position(s), there should be one or two donor atom(s). The different is that the distance between Cu^{2+} and the donor atom is longer than the normal, due to the Jahn–Teller effect for a d^9 Cu^{2+} ion. The Cu1–Clb/Cl1c distance of 3.496 Å is within the accepted range,[17i] indicating that Cl1b and Cl1c occupy the axial potions of Cu1. Therefore, Cu1 is actually in a 4 + 2 site (see Fig. S5† for better understanding). Moreover, in some Cu^{2+} compounds reported previously, longer Cu–Cl distances have been observed.[17i] *Via* the longer Cu1–Cl interactions, the planar $CuCl_4^{2-}$ units are linked into a 2-D single-layer network. Fig. 6c is the polyhedral plot of this 2-D single-layer network. All symmetry-related Cu1 centers adopt a distorted octahedral configuration. *Via* sharing their corners, the Cu^{2+} octahedra are linked into a 2-D single-layer network. This 2-D layer network resembles a classical perovskite single-layer network. The $H_2(cha)^{2+}$ cations occupy the space between the inorganic anion layers (see Fig. 6a).

Structural discussion

With various organic base molecules as the countercations, five new hybrid Cd(II) compounds and one new chlorocuprate (II) were obtained. The anionic Cd–SCN frameworks in compounds **1–5** exhibit different structures: the 1-D linear chain in compound **1**, the 1-D ribbon in compound **2**, the 3-D open framework in compound **3**, the 1-D zigzag chain in compound **4**, and the discrete dimer in compound **5** (see Scheme S1a†). The concept of dimensional reduction and recombination should be employed to understand the formation of these anionic structures.[1c,6c,i,j,17b] In this concept, the Cd–SCN frameworks are thought to derive from the 2-D $Cd(SCN)_2$ layer, in which all of the Cd^{2+} ions are in an octahedral site, and all of the SCN^- groups adopt a triple-bridged coordination mode. The organic base molecule can be visualized as the so-called 'molecular scissors'. With this role for the organic base molecules, the 2-D $Cd(SCN)_2$ layer is cut into the different structures. For example, cut by $H_2(tmen)^{2+}$, a 1-D single chain forms (as observed in **1**), while cut by $H_2(tmba)^{2+}$, a 1-D ribbon forms (as observed in **2**). However, the zigzag chains observed in compounds **3** and **5** are not a slice of the 2-D $Cd(SCN)_2$

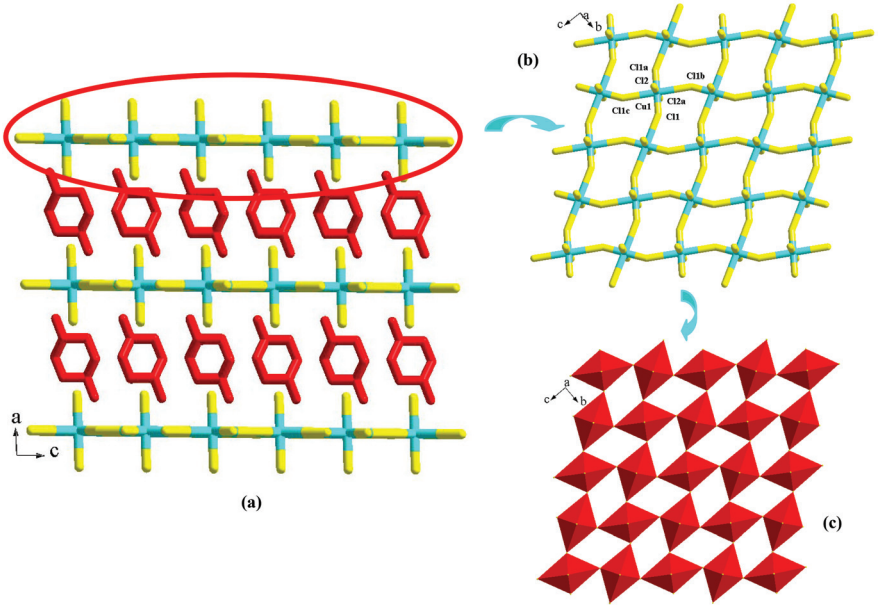

Fig. 6 (a) Projection plot in the (010) direction, and (b, c) 2-D perovskite single-layer network in **6** (a: $-x + 1, -y - 1, -z + 1$; b: $-x + 1, y - 1/2, -z + 1/2$; c: $x, -y - 1/2, z + 1/2$).

layer. This means that the recombination occurs. As shown in Scheme S1b,† the 1-D zigzag chain should originate from the recombination of the 1-D linear chain, in order to form a more stable network. Two structural factors determine that the zigzag chain has a potential to form a 3-D stable network through further interactions, as observed in compounds **3** and **4**: (i) the appearance of the *cis*-configuration $Cd(SCN)_2$ unit and (ii) the alternate distribution of the *cis*-$Cd(SCN)_2$ units on both sides of the zigzag chain. To date, organically templated thiocyanatocadmates with the 3-D structure are rather rare. Only two examples, $[(Hdabco)_2Cd_3(SCN)_8]$ and $[H_2(tmen)][Cd_3Cl_6(SCN)_2]$, have been reported.[14,15] Besides the role of $H(abp)^+$, the formation of the dimer in compound **5** should derive from the incorporation of $[H(abp)]_2SO_4$. This situation has also occurred in the past investigation. For example, compound $[H_2(4,4'\text{-dtdpy})][Cd_2Br_6]$ possesses a 1-D ribbon structure,[14] while compound $[H_2(4,4'\text{-dtdpy})]_2[CdBr_4]SO_4{\cdot}2.5H_2O$, a double salt of $[H_2(4,4'\text{-dtdpy})][CdBr_4]{\cdot}[H_2(4,4'\text{-dtdpy})]_2SO_4$, only exhibits a mononuclear structure.[16a] Moreover, based on the supramolecular structures of compounds **1** and **2** (see Fig. S6†), we find that the number of C atoms between the two N atoms in the templating agent controls the width of the 1-D linear chain. With the increase of the number of C atoms from 2 (tmen) to 4 (tmba), the width of the chain increases from 1 (single chain) to 2 (double chain).

Characterization

The TG behaviors of the title compounds were investigated. Fig. 7 plots the temperature *vs*. weight-loss curves. Compounds **1** and **2** underwent two steps of similar weight loss. In the first step, the countercation is lost in the form of ammonium thiocyanate. The observed weight loss (44% for **1**, 55% for **2**) is lower than that calculated (50.1% for **1**, 64.3% for **2**), indicating that the part intermediates $Cd(SCN)_2$ had transformed into CdO. Therefore, the actual intermediate is a double compound $x\text{Cd(SCN)}_2{\cdot}y\text{CdO}$. The final residues for both are proved to be CdO (Calcd: 27.7%, Found: 28.4% for **1**; Calcd: 35.7%, Found: 35.6% for **2**), suggesting that $Cd(SCN)_2$ thoroughly transformed into CdO in the second step of weight loss. Compound **4** underwent three steps of weight loss. The initial two steps of weight loss are assigned to the sequential sublimation of amp and CH_3COOH. At the same time, a little $Cd(SCN)_2$ intermediate transformed into CdO. Therefore, the intermediate is a

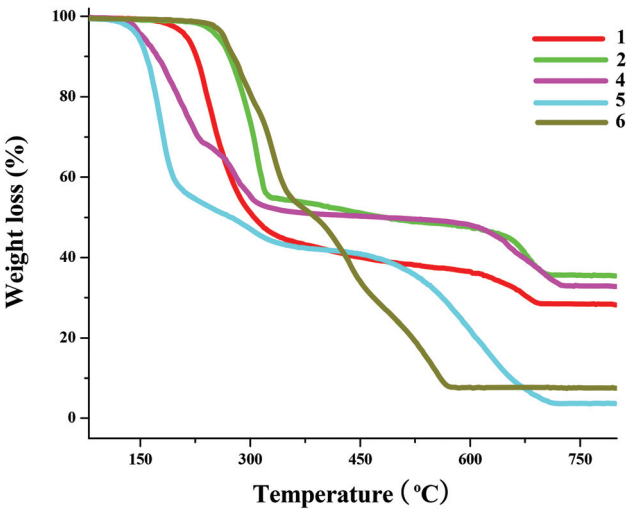

Fig. 7 TG curves of title compounds.

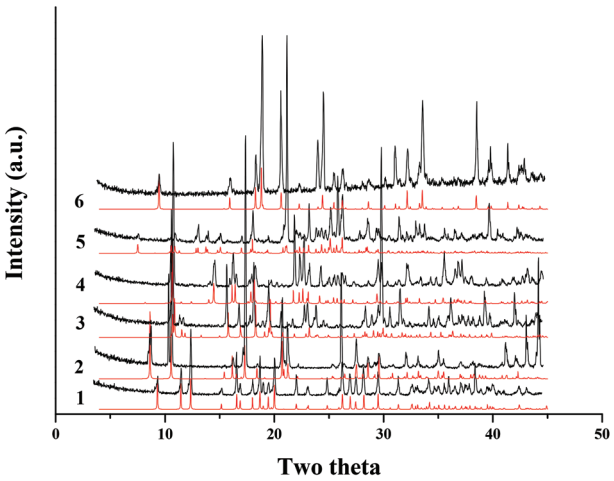

Fig. 8 Powder XRD patterns of the title compounds.

double compound of $Cd(SCN)_2$ and CdO after two steps of weight loss. The remainder is still CdO, and the calculated value of 32.4% is comparable with that observed (33.0%). Compound **5** also underwent three steps of weight loss. The *ca.* 41.0% weight loss for the first step is attributed to the removal of $[H(abp)]_2SO_4{\cdot}H_2O$ (Calcd: 40.0%). At this time, the intermediate is $[H(abp)]_2[Cd(SCN)_4]$. The residue content of 4.11% implies that during the weight loss process, some Cd evaporated. Based on the previous related investigation, $Cd(SCN)_2$ does not evaporate generally at high temperature, but $CdBr_2$ is frequently found to evaporate upon heating.[12–16] Therefore, we speculate that during the weight loss process, the intermediate $CdBr_2{\cdot}Cd(SCN)_2$ should form. The Br^- ion came from abp. Upon further heating, $CdBr_2$ evaporated completely, and $Cd(SCN)_2$ transformed to CdO. The residue content is calculated to be 5.56%, which is comparable with that observed. Different from the situation of CdX_2, part of the $CuCl_2$ transformed into CuO along with the evaporation of $CuCl_2$. Therefore, the residue content for compound **6** is 7.5%, rather than zero. In the title compounds, compounds **2** and **6** have the better thermal stability and can be thermally stable up to *ca.* 240 °C.

Fig. 8 plots the experimental and simulated powder XRD patterns of the title compounds. The experimental powder XRD pattern for each compound is in accord with the simulated one generated on the basis of structural data, confirming that the as-synthesized product is a pure. Based on the IR spectra of the title compounds (see Fig. S7†), we know that (i) there exist bridged-SCN^- groups in compounds **1–5**, since peaks larger than 2100 cm^{-1} are observed (2100 cm^{-1} for **1**, 2131 and 2108 cm^{-1} for **2**, 2131 and 2116 cm^{-1} for **3**, 2129 and 2108 cm^{-1} for **4**, 2123 cm^{-1} for **5**);[20] (ii) the appearance of the peaks at 1094, 1078 (ν_3 and ν_4 vibration modes for SO_4^{2-}) and 982 cm^{-1} (ν_1 mode for SO_4^{2-}) suggest that SO_4^{2-} is mixed in the final framework of compound **5**;[21] (iii) the appearance of peaks at 1669 ($\nu_{as}(COO^-)$) and 1416 cm^{-1} ($\nu_s(COO^-)$) indicates that CH_3COO^- is incorporated in the resulting backbone of compound **4**.[22] These results are in agreement with those obtained from X-ray single-crystal diffraction analysis.

Photoluminescence property

The photoluminescence properties of the five Cd^{2+} hybrids were investigated. In order to compare the emission intensities of the compounds, the same slit widths were used when all were measured. Fig. 9 plots the photoluminescence spectra of compounds **4** and **5**. Obviously, compounds **4** and **5** possess photoluminescence properties. Upon excitation at 335 nm, compound **4** exhibits a violet light emission centered at 365 nm (Fig. 9a), while upon excitation at 395 nm, compound **5** emits a different blue-green light, and the maximum appears at 470 nm (Fig. 9b). The emissions for compounds **4** and **5** are strong, and can be seen clearly under the UV lamp (see the inserted images). Based on the images, we find that the emission intensity of compound **4** is apparently stronger than that of compound **5**, which is in agreement with the conclusion drawn from their emission spectra. In order to reveal the emission mechanism of the two hybrids, the photoluminescence behaviors of the amp and abp molecules were also studied. As shown in Fig. S8,† the amp molecule emits green light (λ_{em} = 495 nm) when excited at 410 nm, whereas the abp molecule emits violet light (λ_{em} = 390 nm) when excited at 360 nm. Only the substituent group at the 6-position is different (–CH_3 for amp, –Br for abp) but the two organic molecules show distinct emission behaviors. Compared with the emission of the corresponding organic molecule, the emission of compound **4** shows a larger blue shift (130 nm), whereas the emission of compound **5** shows a larger red shift (80 nm). Although a larger shift is observed, the emission of compounds **4** and **5**

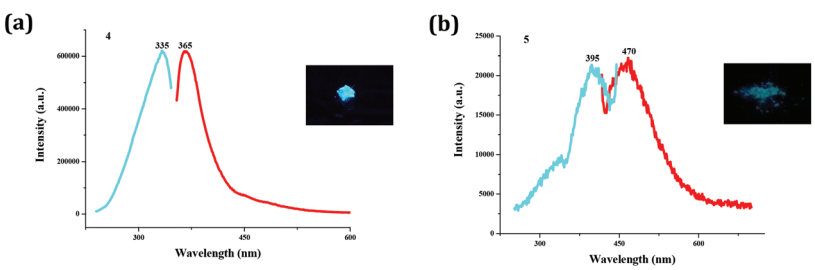

Fig. 9 Photoluminescence spectra of (a) **4** and (b) **5** (inserted images are corresponding emissions under UV lamp).

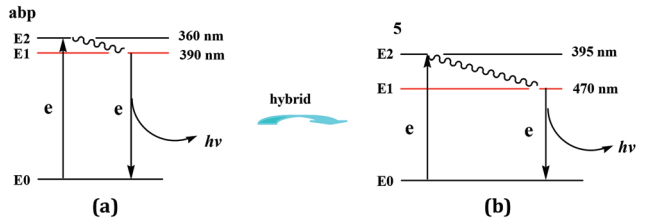

Fig. 10 Diagrams of energy levels of (a) abp and (b) corresponding hybrid **5**.

should be tentatively attributed to the ligand-centered electronic excitation ($\pi^* \rightarrow \pi$). In the previous related reports, this larger shift has also been observed.[15] Since the emission of the amp molecule is lower in energy (495 nm), this is not the original emission from the amp molecule. The green light emission should originate from the trap sites in the crystal.

In order to reveal the effect of the hybrid formation on the photoluminescence behavior of the compound, the diagrams of the energy levels of the abp molecule and compound **5** are drawn in Fig. 10, based on their photoluminescence spectra.[23] As shown in Fig. 10a, when excited at 360 nm, the electron transfers from the ground-state E0 to the excited-stated E2. It then decays nonradiatively to the E1 energy level (the highest occupied molecular orbital, HOMO). From the E1 energy level, the electron returns to the ground-state E0 energy level with light emission (390 nm), and thus the abp molecule emits violet light. After a hybrid formation, the energy level value of HOMO decreases from 390 nm to 470 nm, thus a red shift occurs and compound **5** emits blue-green light (see Fig. 10b). The emission of the amp molecule is too small to be discussed, so only the energy level diagram of compound **4** is drawn (see Fig. S9†). Compounds **1**, **2**, and **3** do not emit light. Based on their solid-state UV-vis spectra (see Fig. S10†), we find that the electron can be excited to the excited state energy level E2. However, due to lack of a π-conjugated structure in the organic molecule, the electron in the HOMO returns to the ground state energy level, E0, in a nonradiative way. Hence, compounds **1**, **2** and **3** do not emit light. Moreover, the composition of the HOMO also has the possibility to be changed after hybrid formation. Once this situation occurs, the emission for the hybrid compound will be assigned to a new attribution.[24]

The emission intensity can also be changed after a hybrid formation. The emission intensity of compound **4** is apparently stronger than that of the amp molecule, while the emission intensity of compound **5** is slightly weaker than that of the abp molecule. On the one hand, due to a hybrid formation, some hydrogen-bond interactions appear in the packing structure of the compound. This provides a possible path for the excited state proton to transfer. The occurrence of the intra-(inter)molecular excited state proton transfer (IEXPT) can significantly enhance or quench the emission of the compound.[25] On the other hand, the hybrid formation can alter the molecular packing of the compound. The molecular packing makes another important impact on influencing the emission behavior of the compound.[26] The close packing of the molecules completely quenches the emission of the compound. In nature, the hybrid formation changes the quantum yield, so the emission intensity for the hybrid compound is different from that of the corresponding organic molecule.

Based on the photoluminescence behaviors of the title compounds and previous related reports,[12–16] we know that (i) some aromatic base-templated thiocyanatocadmates emit light, while due to lack of a π-conjugated structure in the organic molecule, the aliphatic amine-templated thiocyanatocadmates do not emit light; (ii) since the emission originates from ligand-centered electronic excitations, they generally emit high-energy blue or violet light; (iii) the hybrid formation influences the photoluminescence behavior of the hybrid compound. The hybrid formation can alter the energy level of the HOMO, with a result that the hybrid compound may emit different light. Hybrid formation can lead to the appearance of the excited state proton transfer path as well as the change of the molecular packing, indirectly altering the emission behavior of the hybrid compound. The decay curve for compound **4** fits into a double exponential function, and the lifetimes were calculated to be τ_1 = 2.26 ns and τ_2 = 12.21 ns, respectively. The luminescence lifetime for compound **5** was calculated to be τ_1 = 1.16 ns and τ_2 = 3.22 ns, respectively (see Fig. S11†).

Conclusion

In summary, we report the synthesis and structural characterization of five new thiocyanatocadmates and one new chlorocuprate(II). Based on the structural information of compounds **1–5**, we know that with different organic base molecules as the countercations, the inorganic anions can form various structures. The concept of the dimensional reduction and recombination can be employed to better understand the formation of these structures. The organic base molecule serves as the so-called molecular scissors, cutting the 2-D $Cd(SCN)_2$ layer into a 1-D ribbon (in **2**) or a 1-D linear chain (in **1**). With the limitation of ammonium sulfate, the Cd–SCN oligomer can be further cut into a discrete structure (the dimer in **5**). The 1-D zigzag chain derives from the recombination of the 1-D linear chain, in order to form a more stable network as a 3-D open framework (in **3**) or a 3-D supramolecular network (in **4**). The number of C atoms between the two N atoms in the templating agent may control the width of the inorganic anion chain. The photoluminescence analysis reveals that the aromatic base-templated thiocyanatocadmate may emit light, which is generally assigned to the ligand-centered electronic excitation ($\pi^* \rightarrow \pi$). After hybrid formation, (i) the energy level of the HOMO may change; (ii) a transfer path for the excited-state proton may appear; and (iii) the molecular packing may change. Therefore, an organic–inorganic hybrid may show a different emission, compared with the emission of the corresponding organic base molecule. In addition, compound **3** possesses a 3-D open-framework structure. To date, the 3-D

thiocyanatocadmate is rather rare. Compound **6** shows a 2-D perovskite single-layer structure.

Acknowledgements

This research was supported by the National Natural Science Foundation of China (No. 21271083).

References

1 (*a*) D. B. Mitzi, *J. Chem. Soc., Dalton Trans.*, 2001, 1; (*b*) S. P. Zhao and X. M. Ren, *Dalton Trans.*, 2011, **40**, 8261; (*c*) N. Mercier, N. Louvain and W. Bi, *CrystEngComm*, 2009, **11**, 720; (*d*) L. M. Wu, X. T. Wu and L. Chen, *Coord. Chem. Rev.*, 2009, **253**, 2787; (*e*) H. Zhang, X. Wang, K. Zhang and B. K. Teo, *Coord. Chem. Rev.*, 1999, **183**, 157; (*f*) R. Peng, M. Li and D. Li, *Coord. Chem. Rev.*, 2010, **254**, 1.

2 (*a*) T. Yu, L. Zhang, J. Shen, Y. Fu and Y. Fu, *Dalton Trans.*, 2014, **43**, 13115; (*b*) Y. Takahashi, P. Obara, Z. Z. Lin, Y. Takahashi, T. Naito, T. Inabe, S. Ishibashi and K. Terakura, *Dalton Trans.*, 2011, **40**, 5563; (*c*) W. Q. Liao, H. Y. Ye, D. W. Fu, P. F. Li, L. Z. Chen and Y. Zhang, *Inorg. Chem.*, 2014, **53**, 11146; (*d*) L. Z. Cai, M. S. Wang, M. J. Zhang, G. E. Wang, G. C. Guo and J. S. Huang, *CrystEngComm*, 2012, **14**, 6196; (*e*) Y. Z. Qiao, J. M. Yue, X. C. Liu and Y. Y. Niu, *CrystEngComm*, 2011, **13**, 6885; (*f*) M. Tuikka, Ü. Kersen and M. Haukka, *CrystEngComm*, 2013, **15**, 6177; (*g*) E. R. Williams and M. T. Weller, *CrystEngComm*, 2013, **15**, 31; (*h*) B. Andriyevsky, K. Dorywalsky, M. Jaskólski, Z. Czapla, A. Patryn and N. Esser, *Mater. Chem. Phys.*, 2013, **139**, 770; (*i*) Y. Jin, C. H. Yu, W. X. Wang, S. C. Li and W. Zhang, *Inorg. Chim. Acta*, 2014, **413**, 97; (*j*) Q. Hou, F. Q. Bai, M. J. Jia, J. Jin, J. H. Yu and J. Q. Xu, *CrystEngComm*, 2012, **14**, 4000; (*k*) M. L. Liu, *Acta Crystallogr., Sect. C: Cryst. Struct. Commun.*, 2013, **69**, 1128; (*l*) A. Gagor, A. Wakowska, Z. Czapla and S. Dacko, *Acta Crystallogr., Sect. B: Struct. Sci.*, 2011, **67**, 122; (*m*) R. Hajji, A. Oueslati, N. Errien and F. Hlel, *Polyhedron*, 2013, **79**, 97; (*n*) Z. Yu, K. Yu, L. Lai, K. A. Udachin, H. Zhu, J. Tao, X. You, M. Ströbele, H.-J. Meyer and J. A. Ripmeester, *Chem. Commun.*, 2004, 648; (*o*) J. D. Lin, S. H. Wang, L. Z. Cai, F. K. Zheng, G. C. Guo and J. S. Huang, *CrystEngComm*, 2013, **15**, 903; (*p*) G. Paul, A. Choudhury and C. N. R. Rao, *Dalton Trans.*, 2002, 3859; (*q*) J. D. Martin and K. B. Greenwood, *Angew. Chem., Int. Ed. Engl.*, 1997, **36**, 2072.

3 H. Hartl and J. Fuchs, *Angew. Chem., Int. Ed. Engl.*, 1986, **25**, 569.

4 J. R. D. DeBord, Y. J. Lu, C. J. Warren, R. C. Haushalter and J. Zubieta, *Chem. Commun.*, 1997, 1365.

5 Z. J. Zhang, S. X. Xiang, G. C. Guo, G. Xu, M. S. Wang, J. P. Zou, S. P. Guo and J. S. Huang, *Angew. Chem., Int. Ed.*, 2008, **47**, 4149.

6 (*a*) J. A. Barreda-Argüeso, L. Nataf, Y. Rodríguez-Lazcano, F. Aguado, J. González, R. Valiente, F. Rodríguez, H. Wilhelm and A. P. Jephcoat, *Inorg. Chem.*, 2014, **53**, 10708; (*b*) A. E. Maughan, J. A. Kurzman and J. R. Neilson, *Inorg. Chem.*, 2015, **54**, 370; (*c*) A. Thorn, R. D. Willett and B. Twamley, *Cryst. Growth Des.*, 2005, **5**, 673; (*d*) A. Hazari, L. K. Das, A. Bauzá, A. Frontera and A. Ghosh, *Dalton Trans.*, 2014, **43**, 8007; (*e*) S. M. Mobin, V. Mishra, A. Chaudhary, D. K. Rai, A. A. Golov and P. Mathur, *Cryst. Growth Des.*, 2014, **14**, 4124; (*f*) C. E. Costin-Hogan, C. L. Chen, E. Hughes, A. Pickett, R. Valencia, N. P. Rath and A. M. Beatty, *CrystEngComm*, 2008, **10**, 1910; (*g*) C. H. Arnby, S. Jagner and I. Dance, *CrystEngComm*, 2004, **6**, 257; (*h*) L. Subramanian and R. Hoffmann, *Inorg. Chem.*, 1992, **31**, 1021; (*i*) A. B. Corradi, A. M. Ferrari and G. C. Pellacani, *Inorg. Chim. Acta*, 1998, **272**, 252; (*j*) A. A. Thorn, R. D. Willett and B. Twamley, *Inorg. Chem.*, 2008, **47**, 5775; (*k*) M. Bujak, *Cryst. Growth Des.*, 2015, **15**, 1295.

7 (*a*) E. T. Spielberg, E. Edengeiser, B. Mallick, M. Havenith and A.-V. Mudring, *Chem. – Eur. J.*, 2014, **20**, 5338; (*b*) M. Owczarek, P. Szklarz, R. Jakubas and A. Miniewicz, *Dalton Trans.*, 2012, **41**, 7285; (*c*) F. Coleman, G. Feng, R. W. Murphy, P. Nockemann, K. R. Seddon and M. Swadźba-Kwaśny, *Dalton Trans.*, 2013, **42**, 5025; (*d*) M. Owczarek, R. Jakubas, A. Pietraszko, W. Medycki and J. Baran, *Dalton Trans.*, 2013, **42**, 15069; (*e*) T. Yu, L. An, L. Zhang, J. Shen, Y. Fu and Y. Fu, *Cryst. Growth Des.*, 2014, **14**, 3875; (*f*) C. C. Stoumpos, C. D. Malliakas and M. G. Kanatzidis, *Inorg. Chem.*, 2013, **52**, 9019; (*g*) W. Q. Liao, G. Q. Mei, H. Y. Ye, Y. X. Mei and Y. Zhang, *Inorg. Chem.*, 2014, **53**, 8913.

8 (*a*) J. J. Hou, S. L. Li, C. R. Li and X. M. Zhang, *Dalton Trans.*, 2010, **39**, 2701; (*b*) J. Song, Y. Hou, L. Zhang and Y. Fu, *CrystEngComm*, 2011, **13**, 3750; (*c*) D. P. Jiang, R. X. Yao, F. Ji and X. M. Zhang, *Eur. J. Inorg. Chem.*, 2013, 556; (*d*) S. Sun, L. J. Liu, W. Y. Zhou, J. Li and F. X. Zhang, *J. Solid State Chem.*, 2015, **225**, 1; (*e*) L. Zhang, J. Zhang, Z. J. Li, J. K. Chen, P. X. Yin and Y. G. Yao, *Inorg. Chem.*, 2007, **46**, 5838; (*f*) X. Gao, Q. G. Zhai, S. N. Li, R. Xia, H. J. Xiang, Y. C. Jiang and M. C. Hu, *J. Solid State Chem.*, 2010, **183**, 1150; (*g*) J. J. Zhao, X. Zhang, Y. N. Wang, H. L. Jia, J. H. Yu and J. Q. Xu, *J. Solid State Chem.*, 2013, **207**, 152.

9 (*a*) R. Bhattacharya, A. Ghosh, M. S. Ray, L. Righi, G. Bocelli, S. Chaudhuri, R. D. Willett, J. M. Clemente-Juan, E. Coronado and C. J. Goméz-Garcia, *Eur. J. Inorg. Chem.*, 2003, 4253; (*b*) R. D. Willett, C. J. Gómez-García and B. Twamley, *Eur. J. Inorg. Chem.*, 2012, 3342; (*c*) W. Ouellette, A. V. Prosvirin, V. Chieffo, K. R. Dunbar, B. Hudson and J. Zubieta, *Inorg. Chem.*, 2006, **45**, 9346; (*d*) T. Chivers, Z. Fu and L. K. Thompson, *Chem. Commun.*, 2005, 2339; (*e*) R. D. Willett, B. Twamley, W. Montfrooij, G. E. Granroth, S. E. Nagler, D. W. Hall, J.-H. Park, B. C. Watson and M. W. Meisel, *Inorg. Chem.*, 2006, **45**, 7689; (*f*) R. D. Willett, C. Galeriu, C. P. Landee,

M. M. Turnbull and B. Twamley, *Inorg. Chem.*, 2004, **43**, 3804; (*g*) R. D. Willett, C. J. Gómez-García and B. Twamley, *Polyhedron*, 2005, **24**, 2293; (*h*) M. M. Liu, J. J. Hou, Z. Qi, L. N. Duan, W. J. Ji, C. Han and X. M. Zhang, *Inorg. Chem.*, 2014, **53**, 4130.

10 (*a*) R. G. Lin, G. Xu, G. Lu, M. S. Wang, P. X. Li and G. C. Guo, *Inorg. Chem.*, 2014, **53**, 5538; (*b*) O. Toma, N. Mercier and C. Botta, *Eur. J. Inorg. Chem.*, 2013, 1113; (*c*) N. Mercier, *Eur. J. Inorg. Chem.*, 2013, 1113; (*d*) G. Xu, G. C. Guo, J. S. Guo, S. P. Guo, X. M. Jiang, C. Yang, M. S. Wang and Z. J. Zhang, *Dalton Trans.*, 2010, **39**, 8688.

11 (*a*) J. H. Yu, K. Mereiter, N. Hassan, C. Feldgitscher and W. Linert, *Cryst. Growth Des.*, 2008, **8**, 1535; (*b*) H. Y. Bie, J. Lu, J. H. Yu, J. Q. Xu, K. Zhao and X. Zhang, *J. Solid State Chem.*, 2005, **178**, 1445; (*c*) T. G. Wang, S. Li, J. H. Yu and J. Q. Xu, *Solid State Sci.*, 2015, **41**, 25.

12 H. L. Jia, M. J. Jia, H. Ding, J. H. Yu, J. Jin, J. J. Zhao and J. Q. Xu, *CrystEngComm*, 2012, **14**, 8000.

13 H. L. Jia, M. J. Jia, G. H. Li, Y. N. Wang, J. H. Yu and J. Q. Xu, *Dalton Trans.*, 2013, **42**, 6429.

14 H. L. Jia, G. H. Li, H. Ding, Z. M. Gao, G. Zeng, J. H. Yu and J. Q. Xu, *RSC Adv.*, 2013, **3**, 16416.

15 B. Guo, X. Zhang, Y. N. Wang, J. J. Huang, J. H. Yu and J. Q. Xu, *Dalton Trans.*, 2015, **44**, 5095.

16 (*a*) H. L. Jia, Z. Shi, Q. F. Yang, J. H. Yu and J. Q. Xu, *Dalton Trans.*, 2014, **43**, 5806; (*b*) H. L. Jia, M. J. Jia, G. Zeng, J. Jin, J. H. Yu and J. Q. Xu, *CrystEngComm*, 2012, **14**, 6599; (*c*) J. Jin, M. J. Jia, Y. Peng, J. H. Yu and J. Q. Xu, *CrystEngComm*, 2011, **13**, 2942; (*d*) J. H. Yu, X. M. Wang, L. Ye, Q. Hou, Q. F. Yang and J. Q. Xu, *CrystEngComm*, 2009, **11**, 1037.

17 (*a*) F. F. Awwadi, S. F. Haddad, M. M. Turnbull, C. P. Landee and R. D. Willett, *CrystEngComm*, 2013, **15**, 3111; (*b*) A. A. Thorn, R. D. Willett and B. Twamley, *Inorg. Chem.*, 2008, **47**, 5775; (*c*) R. Kapoor, A. Kataria, P. Venugopalan, P. Kapoor, M. Corbella, M. Rodríguez, I. Romero and A. LIobet, *Inorg. Chem.*, 2004, **43**, 6699; (*d*) J. D. Martin, J. Yang and A. M. Dattelbaum, *Chem. Mater.*, 2001, **13**, 392; (*e*) F. Awwadi, R. D. Willett and B. Twamley, *Cryst. Growth Des.*, 2011, **11**, 5316; (*f*) F. F. Awwadi, S. F. Haddad, B. Twamley and R. D. Willett, *CrystEngComm*, 2012, **14**, 6761; (*g*) A. Kessentini, M. Belhouchet, Y. Abid, C. Minot and T. Mhiri, *Spectrochim. Acta, Part A*, 2014, **12**, 476; (*h*) A. K. Vishwakarma, P. S. Ghalsasi, A. Navamoney, Y. Lan and A. K. Powell, *Polyhedron*, 2011, **30**, 1565; (*i*) J. H. Yu, Z. L. Lü, J. Q. Xu, H. Y. Bie, J. Lu and X. Zhang, *New J. Chem.*, 2004, **280**, 940.

18 G. M. Sheldrick, *Acta Crystallogr., Sect. A: Found. Crystallogr.*, 2008, **64**, 112.

19 B. Guo and J. H. Yu, Unpublished.

20 (*a*) L. Yi, B. Ding, B. Zhao, P. Cheng, D. Z. Liao, S. P. Yan and J. H. Jiang, *Inorg. Chem.*, 2004, **43**, 33; (*b*) L. Shen and Y. Z. Xu, *J. Chem. Soc., Dalton Trans.*, 2001, 3413.

21 (*a*) M. B. Salah, S. Vilminor, T. Mhiri and M. Kurmoo, *Eur. J. Inorg. Chem.*, 2004, 2272; (*b*) M. B. Salah, S. Vilminor, G. André, M. Richard-Plouet, F. Bourée-Vigneron, T. Mhiri and M. Kurmoo, *Chem. – Eur. J.*, 2004, **10**, 2048.

22 L. J. Zhang, J. Q. Xu, Z. Shi, W. Xu and T. G. Wang, *Dalton Trans.*, 2003, 1148.

23 J. Lu, K. Zhao, Q. R. Fang, J. Q. Xu, J. H. Yu, X. Zhang, H. Y. Bie and T. G. Wang, *Cryst. Growth Des.*, 2005, **5**, 1091.

24 (*a*) J. Jin, F. Q. Bai, M. J. Jia, Y. N. Wang, H. L. Jia, J. H. Yu and J. Q. Xu, *Dalton Trans.*, 2013, **42**, 8771; (*b*) Y. N. Wang, G. H. Li, F. Q. Bai, J. H. Yu and J. Q. Xu, *Dalton Trans.*, 2014, **43**, 15617.

25 (*a*) K. Gavvala, A. Sengupta, R. K. Koninti and P. Hazra, *ChemPhysChem*, 2013, **14**, 3375; (*b*) W. Yang and X. Chen, *Phys. Chem. Chem. Phys.*, 2014, **16**, 4242.

26 (*a*) Y. N. Wang, F. Q. Bai, J. H. Yu and J. Q. Xu, *Dalton Trans.*, 2013, **42**, 16547; (*b*) Y. N. Wang, Q. F. Yang, G. H. Li, P. Zhang, J. H. Yu and J. Q. Xu, *Dalton Trans.*, 2014, **43**, 11646.

